Proceedings of the ASME 2007 International Design Engineering Technical Conferences & Computers and Information in Engineering Conference
IDETC/CIE 2007
September 4-7, 2007, Las Vegas, Nevada, USA

DETC2007-35001

A NOVEL CAPACITIVE DETECTION SCHEME WITH INHERENT SELF-CALIBRATION

Alexander A. Trusov*
MicroSystems Laboratory
Dept. of Mechanical and Aerospace Engineering
University of California, Irvine
Irvine, CA 92697-3975
Email: atrusov@uci.edu

Andrei M. Shkel
MicroSystems Laboratory
Dept. of Mechanical and Aerospace Engineering
University of California, Irvine
Irvine, CA 92697-3975
Email: ashkel@uci.edu

ABSTRACT

This paper reports a novel capacitive detection method which is robust to variations of such critical parameters as the nominal capacitance, frequency and amplitude of the probing voltage, and gain of the trans-impedance amplifier. The approach constructively utilizes inherent nonlinearity of parallel plate sense capacitors in order to measure amplitude of sinusoidal motion. In the case of parallel plate detection signal, multiple harmonics exist and carry redundant information about the amplitude of mechanical motion. The amplitude of motion can be extracted from the ratio of two simultaneously measured harmonics. The paper presents details of a real-time measurement algorithm. Functionality of the algorithm is confirmed by simulations and experiments. The technique is especially valuable for capacitive detection and self-calibration in resonant structures, such as gyroscopes, resonant microbalances, and chemical sensors.

1 INTRODUCTION

Several important classes of MEMS devices, such as resonators [1], gyroscopes [2], and chemical sensors [3] rely on resonance phenomenon in their operation. In these devices, resonant motion needs to be actuated, sensed, and controlled. This paper focuses on capacitive detection of vibratory motion. Conventional capacitive detection schemes produce a signal proportional to such system parameters as nominal sense capacitance, carrier voltage amplitude and frequency, and gain of the current amplifier. These dependencies constitute a need to calibrate individual MEMS devices to address fabrication imperfections, and fluctuation of the parameters due to changing environment and aging. A detection technique independent of these system parameters can be of great advantage.

Capacitive detection of sinusoidal motion is often based on measuring the current induced by the relative motion of the capacitive electrodes. The variable sense capacitor is formed between a mobile mass and anchored electrodes. This capacitor is biased by a certain known DC or AC voltage [4–6]. The motion induced change in capacitance results in the flow of current, which is converted to voltage. This output voltage is detected and related to the motion of the resonant structure.

Electromechanical Amplitude Modulation (EAM) is a widely used capacitive detection approach. It is based on modulation of motional signal by an AC probing voltage (carrier), and allows for frequency domain separation between the informational signals and feed-through of the driving voltages [4, 7]. Conventional linear EAM can be used for either lateral comb sense capacitors or small displacement parallel plate capacitors. In the linear case only one pair of modulated sidebands exist and active calibration of the pick-up signal is needed.

Nonlinear nature of the parallel plate capacitive detection was introduced in [8]. Based on these results, in this paper we report a novel capacitive detection method with inherent self-

*Address all correspondence to this author.

calibration. We first describe a general electro-mechanical model of a resonator with parallel plate capacitive detection in Section 2. The parallel plate EAM pick-up signal is studied in Section 3. Based on the nonlinear features of the nonlinear pick-up signal, a novel multi-sideband measurement approach is formulated in Section 4 and verified experimentally in Section 5. A complete real-time multi-sideband measurement algorithm is reported in Section 6 along with simulation results. Applications of the method to differential EAM and pure DC detection are discussed in Section 7. Section 8 concludes the paper.

2 ELECTROMECHANICAL MODEL

Figure 1 shows a general schematic of a capacitive micro-resonator, a basic element of various dynamic micro-sensors and micro-actuators. The electro-mechanical diagram includes the mechanical resonator, the electrostatic drive and sense electrodes, and a signal processing block which measures the amplitude of motion. The suspended mass of the resonator is constrained to move only along the horizontal x-axis. The variable sense capacitance is defined as $C_s(x)$, and the drive capacitance as $C_d(x)$, where x is the displacement. Typically in MEMS devices, drive and sense terminals are not completely isolated, but are electrically coupled by stray parasitic capacitors and resistors [6]. In this paper we assume, without loss of generality, that the parasitic circuit consists of a single lumped capacitor C_p. An AC driving voltage $V_d(t) = v_d \cos(\omega_d t)$ is applied to the drive electrode (voltage values are referenced with respect to a common ground) to actuate a sinusoidal motion. The sense capacitor C_s is formed between the mobile mass and the fixed sense electrode. The sense electrode is connected to the inverting input of an operational amplifier which is configured as a trans-impedance amplifier, [9].

The oscillatory motion at the drive frequency ω_d is excited by a combination of V_{dc} and V_d driving voltages across the drive capacitor. Without discussing further details of the actuation scheme, resonator's displacement $x(t)$ can be expressed as

$$x(t) = \|x\| \sin(\omega_d t + \phi), \tag{1}$$

where $\phi = \phi(\omega_d)$ represents a phase lag in the transfer function of the resonator.

Due to the harmonically excited motion the sense capacitance $C_s(x)$ changes, causing a flow of motional current $I_s = \frac{d(C_s V_s)}{dt}$, where V_s is the sensing voltage across the sense capacitor. The total pick-up current $I(t) = I_s(t) + I_p(t)$ consists of both the motional and the parasitic currents, and is converted to the final output voltage $V(t)$ with trans-impedance gain $-R$. Parasitic current is induced by the drive voltage V_d and therefore has the same frequency ω_d. In this work we assume that the total sensing voltage $V_s(t) = V_{dc} + V_c(t)$ is composed of a DC component V_{dc}

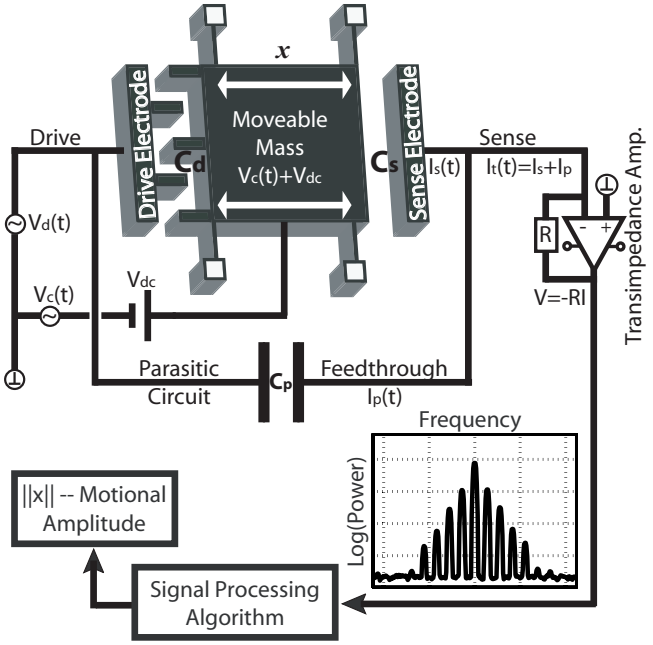

Figure 1. Schematic of a capacitive MEMS resonator with parallel plate detection of motion.

and an AC component $V_c = v_c sin(\omega_c t)$, called carrier. Particular cases when either DC or AC component of the sense voltage is zero are discussed later in this paper. Use of an AC carrier voltage results in an amplitude modulation of the motional signal, known as Electromechanical Amplitude Modulation (EAM).

According to laws of electrostatics, the total pick-up voltage on the output of the current amplifier is

$$V(t) = -R\frac{d}{dt}[V_d(t)C_p + (V_c(t) + V_{dc})C_s(t)]. \tag{2}$$

In Section 3 we expand the pick-up current for the case of parallel plate sense capacitor without using a small displacement assumption.

3 MOTION DETECTION WITH PARALLEL PLATES

This section studies the nonlinear properties of parallel plate EAM pick-up signal. Details are presented in [8] and are summarized here for completeness of the discussion. Consider a variable sense capacitor $C_s(t)$ formed by a pair of mobile and anchored parallel plate structures. Let us denote media permittivity by ε, the initial gap between plates at rest by g, individual parallel plate pair overlap length by L, and plate height (i.e. structural layer thickness) by y. The total overlap area in the sense capacitor is given by $A = NLy$, where N is a number of parallel plate pairs in the capacitor. The total variable sense capacitance for the

harmonic mode of motion (1) is

$$C_s(t) = \frac{\varepsilon A}{g - x(t)} = \frac{\varepsilon A}{g} \frac{1}{1 - \frac{\|x\|}{g} \sin(\omega_d t)}, \tag{3}$$

where the phase of motion ϕ is omitted without any loss of generality.

We introduce nominal sense capacitance $C_{sn} = \frac{\varepsilon A}{g}$ and dimensionless amplitude of motion $x_0 = \|x\|/g < 1$ (normalized with respect to the initial gap between parallel plates). From (3), the sense capacitance is

$$C_s(t) = C_{sn} \frac{1}{1 - x_0 \sin(\omega_d t)}. \tag{4}$$

As shown in [8], the Fourier series representation of the parallel plate capacitance $C_s(t)$ for a given amplitude of motion x_0 is

$$\begin{aligned} C_s(t) = C_{sn} \sum_{k=0}^{\infty} p_{2k}(x_0) \cos(2k\omega_d t) + \\ + C_{sn} \sum_{k=0}^{\infty} p_{2k+1}(x_0) \sin((2k+1)\omega_d t), \end{aligned} \tag{5}$$

where functions $p_k(x_0)$ define the amplitudes of the multiple harmonics in the capacitance $C_s(t)$ and are given by

$$\begin{aligned} p_0(x_0) &= \sum_{n=0}^{\infty} \frac{C(2n,n)}{2^{2n}} x_0^{2n}, \text{ and for k=0,1,2...}\infty \\ p_{2k+1}(x_0) &= (-1)^k \sum_{n=k}^{\infty} \left\{ \frac{C(2n+1, n-k) x_0^{2n+1}}{2^{2n}} \right\} \\ p_{2k}(x_0) &= (-1)^k \sum_{n=k}^{\infty} \left\{ \frac{C(2n, n-k) x_0^{2n}}{2^{2n-1}} \right\}, \end{aligned} \tag{6}$$

where $C(n,k) = \frac{n!}{k!(n-k)!}$ are the Newton's binomial coefficients.

Equation (5) shows that when parallel plates are used to sense the harmonic motion, the time varying sense capacitance contains an infinite number of drive frequency harmonics. In order to calculate the total output signal, we consider modulation of each capacitive harmonic individually. Following [8] we combine the sense capacitance in (5) with (2) to calculate the total output current:

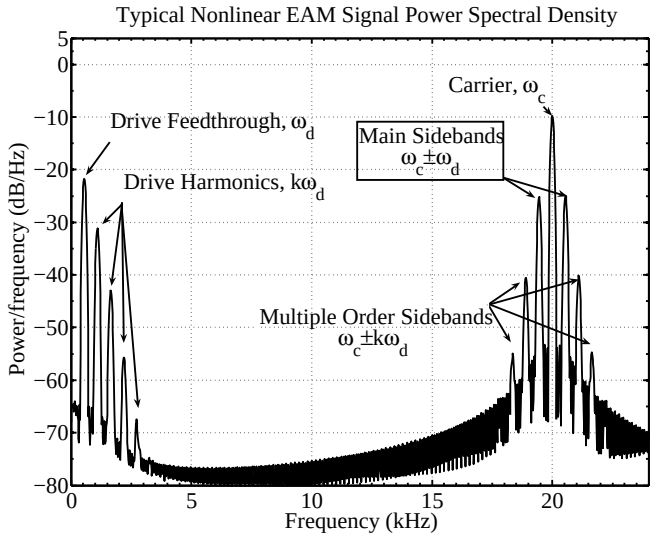

Figure 2. Frequency domain profile of the parallel plate EAM pick-up signal (computer simulation).

$$\begin{aligned} I(t) &= -C_p v_d \omega_d \sin(\omega_d t) + C_{sn} v_c \omega_c p_0(x_0) \cos(\omega_c t) \\ &+ C_{sn} V_{dc} \omega_d \left\{ \begin{array}{c} \sum_{k=0}^{\infty} (2k+1) p_{2k+1}(x_0) \cos((2k+1)\omega_d t) \\ -\sum_{k=1}^{\infty} 2k p_{2k}(x_0) \cos(2k\omega_d t) \end{array} \right\} \\ &+ \frac{1}{2} C_{sn} v_c \left\{ \sum_{k=0}^{\infty} p_{2k+1}(x_0) \left[\begin{array}{c} \omega_{(2k+1)} \sin(\omega_{(2k+1)} t) - \\ -\omega_{-(2k+1)} \sin(\omega_{-(2k+1)} t) \end{array} \right] \right\} \\ &+ \frac{1}{2} C_{sn} v_c \left\{ \sum_{k=1}^{\infty} p_{2k}(x_0) \left[\begin{array}{c} \omega_{(2k)} \cos(\omega_{(2k)}) t) + \\ +\omega_{(-2k)} \cos(\omega_{(-2k)}) t) \end{array} \right] \right\}, \end{aligned} \tag{7}$$

where $\omega_k = \omega_c + k\omega_d$ is the frequency of the k order sideband (left or right, depending on the sign of k). The equation gives the Fourier series for the total pick-up signal for the case of parallel plate capacitive detection of harmonic motion. Figure 2 shows the frequency domain representation of a typical parallel plate EAM pick-up signal and illustrates its important features. The signal contains an infinite number of harmonics corresponding to the drive frequency and multiple informational sidebands.

Let V_ω denote harmonic component of frequency ω of the total output voltage $V = -RI$. According to Eqn. (7), the amplitudes of the right and left sidebands in the total output voltage are given by

$$\|V_{\omega_{\pm k}}\| = \frac{1}{2} R C_{sn} v_c \, |(\omega_c \pm k\omega_d) p_k(x_0)| \,. \tag{8}$$

In practice, a high frequency carrier is usually used [4], [7], so that $\omega_c \gg k\omega_d$ for several first orders $k = 1,\ 2,3...K$. For these

sidebands,

$$\|V_{\omega_{\pm k}}\| = \frac{1}{2} RC_{sn} v_c (\omega_c \pm k\omega_d) \, ||p_k(x_0)|| \approx \tag{9}$$
$$\approx \frac{1}{2} RC_{sn} v_c \omega_c \, ||p_k(x_0)|| .$$

The amplitudes of the multiple sidebands are proportional to functions $p_k(x_0)$, which we call the normalized sidebands amplitudes. It can be shown that a simple closed form expressions for normalized sidebands amplitudes can be derived from Eqn. (6):

$$||p_k(x_0)|| = \frac{1}{\sqrt{1-x_0^2}} \left(\frac{x_0}{(1+\sqrt{1-x_0^2})} \right)^k = \tag{10}$$
$$= 2p_0(x_0) \left(\frac{x_0}{(1+\sqrt{1-x_0^2})} \right)^k .$$

According to this equation, for a fixed motional amplitude x_0, normalized amplitudes of multiple sidebands form a geometric progression with ratio

$$r = ||p_{k+1}(x_0)||/||p_k(x_0)|| = \frac{x_0}{1+\sqrt{1-x_0^2}}. \tag{11}$$

Section 4 discusses how simultaneous demodulation of the multiple sidebands can be used to produce a self-calibrated measurement of the motional amplitude x_0. Section 5 provides experimental confirmation of Eqn. (11).

4 MULTI-SIDEBAND DEMODULATION OF PARALLEL PLATE EAM SIGNAL

In this section we discuss how the ratio of the parallel plate EAM sidebands can be used to robustly detect the motion. First, we review the conventional approach to EAM detection following [4, 7].

4.1 Conventional Linear Approach

In the conventional linear approach (i.e., for lateral comb sense capacitor or parallel plate sense capacitor with small amplitude) only main ($k = 1$) sidebands are considered. Also, the amplitudes of these main sidebands are assumed to be linear with respect to the amplitude of motion, $||V_{\omega_c \pm \omega_d}|| \propto x_0$. In the conventional approach, the extraction of the motional amplitude from the EAM pick up signal consists of amplitude demodulation and scaling steps:

1. Mixing $V(t)$ with phase shifted carrier signal (i.e., multiplication $V(t) \bigotimes sin(\omega_c t)$) to map the sidebands from $\omega_c \pm \omega_d$ to ω_d frequency.
2. Low-pass filtering to attenuate at frequencies higher than ω_d.
3. Mixing the resulting signal with $sin(\omega_d t + \alpha)$ to map the signal from ω_d to DC. Phase α needs to be controlled to match the phase of motion; alternatively, a dual phase I/Q demodulation can be used.
4. The obtained DC signal is scaled by $(RC_{sn} v_c \omega_c)^{-1}$ to calculate the amplitude of mechanical motion.

Consider a resonant MEMS device in which amplitude of motion in certain vibrational mode needs to be detected precisely. In the case of parallel plate sense capacitor, the amplitudes of the informational sidebands are not linear with respect to the amplitude of motion. This nonlinearity introduces significant error if large amplitude of motion is measured. As shown in [8], the amplitude of motion can be measured precisely by adding an additional step to the described demodulation procedure:

$$x_0(p_1) = \frac{\left(w^2 - 12 + p_1^2 - p_1 w\right)\left(w^2 - 12 + p_1^2 + 2pw\right)}{18 p_1 \, w^2},$$
$$\text{where } w = \left(72p_1 - p_1^3 + 6(48 + 132p_1^2 - 3p_1^4)\right)^{\frac{1}{6}}. \tag{12}$$

Both the conventional approach and Eqn. (12) produce the measurement based on the assumed values of such system parameters as trans-resistance gain, nominal capacitance, and carrier voltage. In this case, each device needs to be calibrated to identify these mechanical and electrical parameters. Moreover, during operation, some of these parameters are prone to drifts, causing a loss of the calibration. Approaches based on only the first order sidebands do not provide a robust solution.

4.2 Multi-Sideband Approach

In the case of parallel plate sense capacitors, it is possible to detect arbitrary amplitude of motion without using R, C_{sn}, ω_c and v_c. The approach is based on simultaneous processing of multiple sidebands and produces measurement of x_0 by using the ratio r of magnitudes of two different order sidebands.

According to Eqn. (8) and Eqn. (11), the ratio of amplitudes of any two successive low order sidebands depends only on the amplitude of motion x_0, while all other parameters cancel out:

$$\frac{||V_{\omega_{-(k+1)}}|| + ||V_{\omega_{(k+1)}}||}{||V_{\omega_{-k}}|| + ||V_{\omega_k}||} = \frac{||p_{k+1}(x_0)||}{||p_k(x_0)||} = \tag{13}$$
$$= r(x_0) = \frac{x_0}{(1+\sqrt{1-x_0^2})}.$$

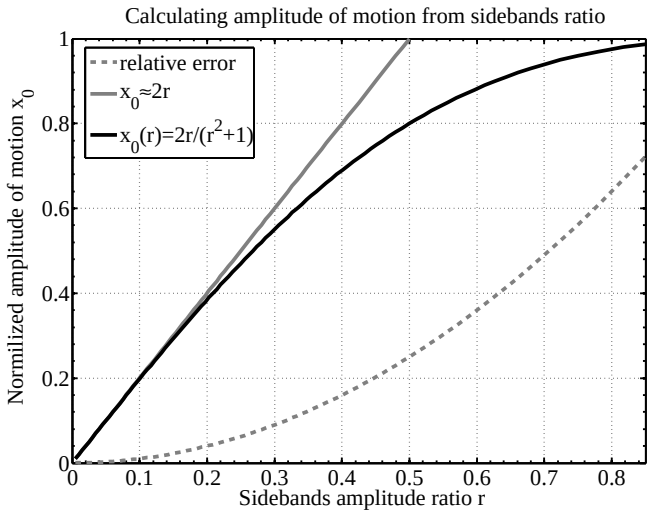

Figure 3. Detection of the amplitude of motion based on the measured ratio of two sidebands amplitudes.

According to Eqn. (9), the same is approximately valid for a ratio of low order single-side sidebands:

$$r(x_0) \approx \frac{||V_{\omega_c \pm (k+1)\omega_d}||}{||V_{\omega_c \pm k\omega_d}||}. \tag{14}$$

There is a simple one-to-one relationship between the amplitude of motion and the amplitude ratio of the two successive parallel plate EAM sidebands. Solving Eqn. (11) for the amplitude of motion yields

$$x_0 = \frac{2r}{r^2+1}. \tag{15}$$

This relationship can be linearized in order to provide a very simple method of x_0 estimation:

$$x_0 \approx \widetilde{x_0} = 2r, \tag{16}$$

with the relative error given by

$$e_{\widetilde{x_0}} = \frac{x_0 - \widetilde{x_0}}{x_0} = r^2. \tag{17}$$

According to this equation, the relative error of linearization $\widetilde{x_0}$ is very small for small amplitudes of motion.

Figure 3 illustrates Eqn. (15), Eqn. (16), and Eqn. (17). In the case of parallel plate EAM detection, normalized amplitude of motion x_0 can be precisely calculated as in Eqn. (15) or estimated by Eqn. (16) based on a single parameter – amplitude ratio of two successive sidebands $r(x_0)$. Feasibility of the proposed measurement technique is demonstrated using experimental data in Section 5.

A real-time detection of motion based on the ratio of sidebands can be performed by the following procedure:

1. Detect amplitude of the first order sidebands at frequencies $\omega_c \pm \omega_d$.
2. Detect amplitude of the second order sidebands at frequencies $\omega_c \pm 2\omega_d$.
3. Calculate the ratio of amplitudes $r = \frac{||V_{\omega_{-2}}||+||V_{\omega_2}||}{||V_{\omega_{-1}}||+||V_{\omega_1}||}$, or estimate using a single side pair of sidebands $r \approx \frac{||V_{\omega_{-2}}||}{||V_{\omega_{-1}}||} \approx \frac{||V_{\omega_2}||}{||V_{\omega_1}||}$.
4. Calculate normalized amplitude of motion $x_0 = \frac{2r}{r^2+1}$.

The first two steps – the demodulation procedures – are performed simultaneously. Demodulation of the first and second order sidebands can be done similarly to the conventional case, described in Section 4.1. A complete real-time signal processing algorithm based on two single side sidebands is presented in Section 6 along with simulation results.

5 EXPERIMENTAL DEMONSTRATION

In order to verify the relationship in Eqn. (15) between amplitude of motion and the ratio of sidebands, test structures were designed, fabricated, and characterized. The devices were capacitive MEMS resonators with lateral comb drive capacitors, and lateral comb and parallel plate sense capacitors. The fabrication was done using an in-house wafer-level SOI process. SOI wafers with a highly conductive 50 μm thick device layer were used. AZ4620 photoresist was spin-coated onto the wafers and patterned using a chrome-on-glass mask and a Karl Suss MA6 exposure system. After photoresist development, the wafers were subjected to a Deep Reactive Ion Etching (DRIE) using a Surface Technology Systems (STS) tool. Minimum gap feature of the process was 5 μm and minimum structural feature was 8 μm. Nominal capacitive gap in the parallel plate sense structure was 25 μm for feasible optical control of the experiments using a microscope. An SEM image of the fabricated test resonator is shown in Figure 4.

During the experiment, the test device was driven into linear vibrations using a lateral comb drive capacitor with a combination of 30 V DC bias with a 3.5 Vrms AC at 555 Hz. An AC carrier voltage of 5 Vrms at 20 kHz was applied to the mobile mass. A parallel plate sense capacitor was connected to a transresistance amplifier, as shown in Figure 1. The voltage output of the amplifier was fed into a dynamic signal analyzer for data capturing and spectral measurements.

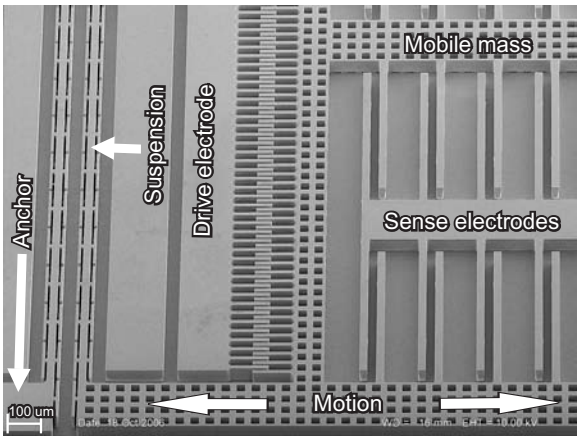

Figure 4. SEM micrograph of a quarter of the fabricated device.

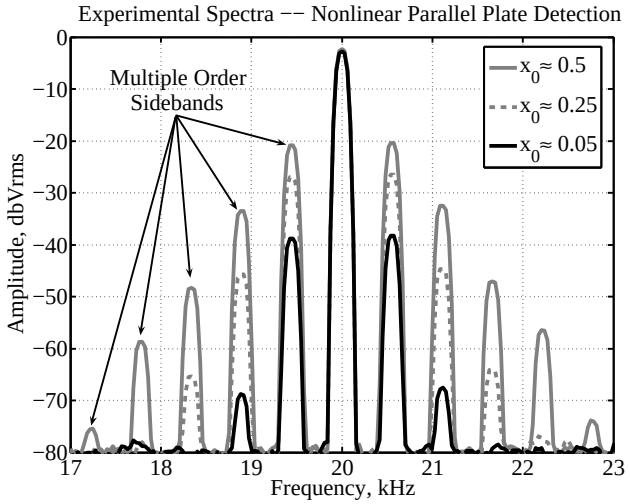

Figure 5. Experimental spectral measurement of the parallel plate EAM pick-up signal at different motional amplitudes.

Figure 5 shows the spectral profile of the generated pick up signal at three different amplitudes of motion, which were visually estimated using a microscope. As expected, multiple sidebands are present in the spectrum, and their amplitudes form a geometric progression (which is seen as a linear decay of amplitudes in the logarithmic scale). Table 1 summarizes these spectral measurements based on sidebands ratio of Eqn. (15). As predicted by the theoretical analysis, the amplitudes of motion are easily obtained from the ratio of subsequent sidebands without using any other system parameters.

6 COMPLETE REAL-TIME ALGORITHM

A real-time measurement algorithm based on Eqn. (14) and Eqn. (15) was developed and simulated using Simulink software.

Table 1. Experimental demonstration of the multi-sideband demodulation: detection of the normalized amplitude of motion x_0 based on the measured sidebands ratio r (see Fig. 5).

visually detected x_0	sidebands ratio r	x_0 calculated by (15)
≈ 0.05	$29.2\ dB = 28.8$	0.07
≈ 0.25	$17.5\ dB = 7.5$	0.26
≈ 0.5	$12\ dB = 4$	0.47

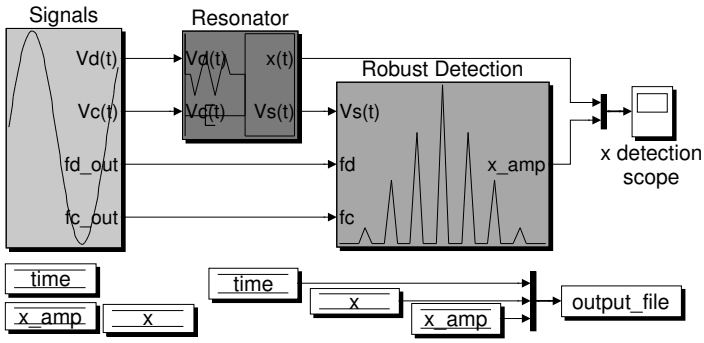

(a) Top level schematic.

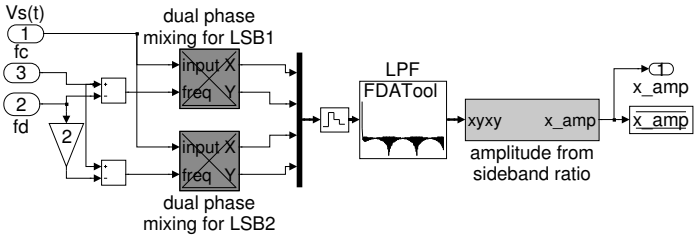

(b) "Robust Detection" block.

Figure 6. Simulink model of a resonator with parallel plate multi-sideband detection scheme.

Figure 6(a) shows the overall view of the Simulink model. It consists of the following high level blocks. The "Signals" block generates drive and carrier voltages. The "Resonator" block represents a capacitive resonator. The outputs of this block are the displacement $x(t)$ and the parallel plate EAM pick up voltage $V_s(t)$. The "Robust Detection" block extracts the amplitude of motion from the ratio of parallel plate EAM sidebands.

Figure 6(b) shows the demodulation procedure, which consists of two steps: amplitude demodulation of two successive sidebands, and calculation of the motional amplitude from the ratio of sidebands amplitudes. The "Robust Detection" block includes dual phase mixing at frequencies of the first and second left sidebands, Fig. 8(a). Extraction of the amplitude of motion according to Eqn. (15) is done by the "x_amp calc" block, Fig. 8(b).

Figures 7(a) and 7(b) show content of the "Signals" and the

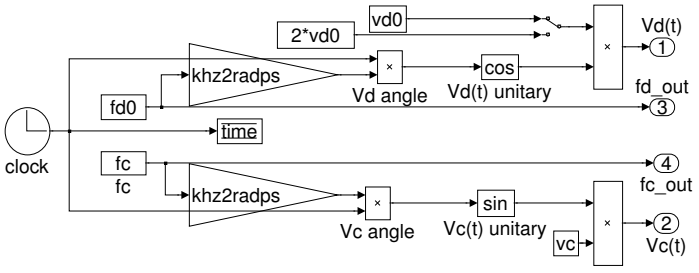

(a) "Signals" block

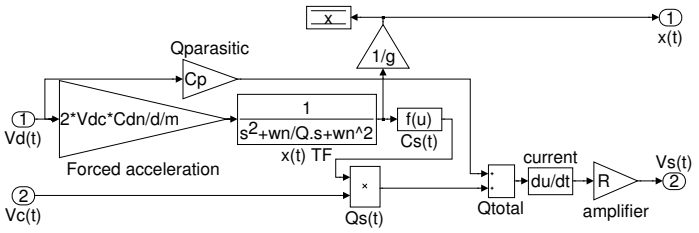

(b) "Resonator" block

Figure 7. Simulink model of a resonator with parallel plate multi-sideband detection scheme.

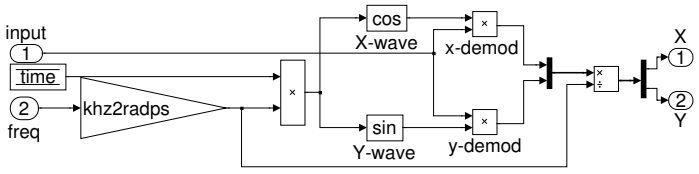

(a) "Dual-phase mixing" block

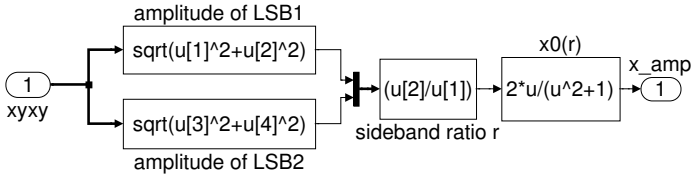

(b) "Amplitude calculation" block

Figure 8. Simulink model of a resonator with parallel plate multi-sideband detection scheme.

"Resonator" blocks of the Simulink model, discussed in Section 6. The "Signals" block generates drive $V_d(t)$ and carrier $V_c(t)$ voltages and a common time reference for the system. In the "Resonator" block, input drive voltage is converted into electrostatic force, which excites the motion. Displacement $x(t)$ is used to calculate the total charge of the parallel plate sense capacitor. The total output current is calculated as a sum of the parasitic and the sense currents. The block outputs the amplified voltage.

The described Simulink model was used to verify feasibility of the proposed real-time detection method. Figure 9 shows

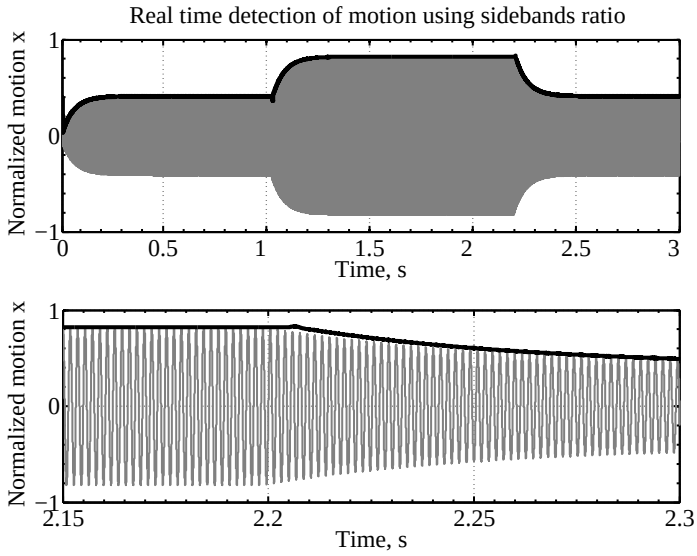

Figure 9. Detection of motional amplitude based on sidebands ratio Eqn. (15), simulation results. The bottom figure is a zoom-in of the top plot. The gray sinusoidal line is the actual normalized motion, and the black envelope line is the result of the multi-sideband demodulation algorithm.

the results of the simulation for a resonator with quality factor $Q = 100$ and natural frequency 555 Hz. The carrier voltage was 2 V_{pk} at 10 kHz. Other simulation parameters include nominal sense capacitance $C_{sn} = 1$ pF, and trans-resistance amplifier gain of 0.5 MΩ. During the simulation the driving AC voltage was switched between 1 V and 2 V amplitudes, causing changes of the motional amplitude. The results of the simulation confirm feasibility of the detection algorithm based on the ratio of sidebands.

7 DISCUSSION

In this section we show how the proposed multi-sideband detection method can be applied to differential EAM and pure DC detection schemes.

7.1 Differential EAM

In the case of differential EAM, even order sidebands cancel out from the total pick-up signal, while odd order sidebands double in amplitude. Similarly to the regular case, the amplitude of motion x_0 is calculated using Eqn. (15); parameter r can be

calculated from the ratio of third and first sidebands according to

$$r(x_0) = \sqrt{\frac{||V_{\omega_{-(k+2)}}|| + ||V_{\omega_{(k+2)}}||}{||V_{\omega_{-k}}|| + ||V_{\omega_k}||}} = \tag{18}$$
$$= \sqrt{\frac{\|p_{k+2}(x_0)\|}{\|p_k(x_0)\|}} \approx \sqrt{\frac{||V_{\omega_{\pm(k+2)}}||}{||V_{\omega_{\pm k}}||}}.$$

7.2 Detection with Pure DC Voltage

In some cases the effect of parasitics is negligible and capacitive detection is done with a purely DC biased sense capacitor [10]. This configuration does not involve any carrier and is described by Eqn. (7) with $v_c = 0$. In this case the total output voltage is given by

$$V(t) = -RC_{sn}V_{dc}\omega_d \sum_{k=1}^{\infty} (-1)^{k+1} k p_k(x_0) cos(k\omega_d t). \tag{19}$$

The information on the amplitude of motion is carried by the harmonics of the drive frequency. In conventional linear approach only the first harmonic is considered and is assumed to be proportional to the amplitude of motion. In the complete nonlinear case, the amplitude x_0 can be calculated based on the ratio of the subsequent harmonics Eqn. (15). In turn, the ratio r is easily obtained from the pick up voltage:

$$r(x_0) = \frac{\|p_{k+1}(x_0)\|}{\|p_k(x_0)\|} = \frac{k\|V_{(k+1)\omega_d}\|}{(k+1)\|V_{k\omega_d}\|} = \frac{\|V_{2\omega_d}\|}{2\|V_{\omega_d}\|}. \tag{20}$$

In the commonly used case of differential detection with DC biased parallel plate sense capacitors, only odd order sidebands are present; the ratio r can be calculated from the total pick up voltage as

$$r(x_0) = \sqrt{\frac{k\|V_{(k+2)\omega_d}\|}{(k+2)\|V_{k\omega_d}\|}} = \sqrt{\frac{\|V_{3\omega_d}\|}{3\|V_{\omega_d}\|}}. \tag{21}$$

For instance, the ratio of the first and third third drive frequency harmonics can be used.

8 CONCLUSIONS

We presented a novel robust method of motion detection in capacitive resonant devices. Feasibility of the proposed multi-sideband approach is supported by experimental results. In the case of parallel plate sense capacitor, the pick-up signal contains multiple nonlinear harmonics of the motional frequency. All these harmonics carry information about the amplitude of motion. The proposed method constructively utilizes nonlinearity of the parallel plate detection signal in order to precisely measure the amplitude of motion without the need for calibration. Unlike conventional approaches, the proposed measurement procedure does not depend on values of such system parameters as nominal capacitance, modulating carrier voltage, and gain of the current amplifier.

The method precisely detects arbitrary amplitude of motion and is applicable to both single-sided and differential schemes with either DC or AC sensing voltages. The method can be implemented using regular operational components, as demonstrated by the simulation results. The proposed algorithms can be used for capacitive detection and automatic self-calibration in resonators, gyroscopes, and other vibratory MEMS.

ACKNOWLEDGMENT

This work was supported by the National Science Foundation Grant CMS-0409923, BEI Technologies contract BEI-36974, and UC Discovery program ELE04-10202.

REFERENCES

[1] Stemme, G., 1991. "Resonant silicon sensors". *IOP Journal of Micromechanics and Microengineering,* **1**, pp. 113–125.

[2] Yazdi, N., Ayazi, F., and Najafi, K., August 1998. "Micromachined inertial sensors". *Proceedings of the IEEE,* **86, no. 8**.

[3] Turner, K. K., and Zhang, W. "Design and analysis of a dynamic mem chemical sensor". *Proceedings of the American Control Conference, Arlington, VA, USA, June 25 - 27, 2001*.

[4] Cao, J., and Nguyen, C.-C. "Drive amplitude dependence of micromechanical resonator series motional resistance". *Digest of Technical Papers, 10-th International Conference on Solid-State Sensors and Actuators, Sendai, Japan, June 7 - 10, 1999*.

[5] Acar, C., and Shkel, A. M., 2005. "Structurally decoupled micromachined gyroscope with post-release capacitance enhancement". *IOP Journal of Micromech. and Microeng.,* **15, no 5**, pp. 1092–1101.

[6] Trusov, A., Acar, C., and Shkel, A. M. "Comparative analysis of distributed mass micromachined gyroscopes".

[7] Cagdaser, B., Jog, A., Last, M., Leibowitz, B. S., Zhou, L., Shelton, E., Pister, K. S., and Bposer, B. E. "Capacitive sense feedback control for mems beam steering mirrors". *Solid-State Sensor, Actuator and Microsystems Workshop, Hilton Head, South Carolina, USA, June 6 - 10, 2004*.

[8] Trusov, A. A., and Shkel, A. M. "Parallel plate capacitive detection of large amplitude motion in MEMS". *Interna-*

tional Conference on Solid State Sensors and Actuators and Microsystems, TRANSDUCERS '07, Lyon, France, June 10 - 14, 2007.

[9] Horowitz, P., and Hill, W., 1989. *The Art of Electronics*. Cambridge University Press.

[10] Geen, J. A., Sherman, S. J., Chang, J. F., and Lewis, S. R., December 2002. "Single-chip surface-micromachined integrated gyroscope with 50 deg/hour root allal variance". *IEEE Journal of Solid-State Circuits*.